



# Consequence assessment of indoor dispersion of sarin—A hypothetical scenario

Monica Endregard\*, B. Anders Pettersson Reif<sup>1</sup>, Thomas Vik, Odd Busmundrud

Norwegian Defence Research Establishment (FFI), NO-2027 Kjeller, Norway

## ARTICLE INFO

### Article history:

Received 12 May 2009

Received in revised form 9 October 2009

Accepted 9 November 2009

Available online 13 November 2009

### Keywords:

Sarin

Indoor dispersion

CFD-modelling

Consequence assessment

Consequence management

## ABSTRACT

The objective of this study is to provide a hypothetical scenario of indoor dispersion of the highly toxic nerve agent sarin in a large building, which can be used as a starting point for discussion, planning, training and exercises for emergency services and responsible authorities. The indoor dispersion has been simulated using a Computational Fluid Dynamics (CFD) approach. Possible consequences have been calculated based on concentration and dose profiles. Mild intoxication effects appear within minutes, while serious injuries and fatalities occur approximately 20 min after release. Anticipated key emergency response challenges are: (i) the time factor due to rapid onset of symptoms, (ii) the large number of casualties, and (iii) the contaminated hazard scene.

© 2009 Elsevier B.V. All rights reserved.

## 1. Introduction

The possible release of toxic chemicals, both in case of severe accidents and intentional use in terrorist actions, calls for appropriate emergency response planning, training and exercises. Identifying and analysing representative scenarios are valuable tools for planning, exercises and evaluation of crisis and consequence management and inter-agency cooperation. Relevant scenarios serve as a basis to identify appropriate protection levels and recommendations regarding organisation, procedures, equipment needs and possible shortcomings. Historical cases of intentional use of toxic chemicals to cause mass casualties are very few, the sarin attack in Tokyo in 1995 by the doomsday cult Aum Shinrikyo being the most infamous [1].

The objectives of this study are to simulate the indoor dispersion of the highly toxic nerve agent sarin in a large convention centre, and analyse the possible effects and anticipated emergency response challenges such as an incident might cause. The attack is assumed to be carried out by break-in into the main ventilation facility. A bottle of sarin is emptied in the ventilation shaft. This particular hypothetical scenario has been chosen for two main reasons. Firstly, the sensitive nature of publication of scenarios calls for

caution. Indoor dispersion of sarin occurred in Tokyo in 1995 [1], and a similar type of scenario is used by the U.S. authorities as one of the national planning scenarios [2]. Hence, a novel scenario is not made public through the present work. Secondly, sarin constitutes a representative example of a highly toxic, odour- and colourless, volatile nerve agent, causing rapid onset of symptoms even upon exposure to low concentrations, and thus serves as an interesting and challenging case for emergency personnel.

Indoor transport of contaminants is governed by a range of complex physical processes. Computational Fluid Dynamics (CFD), which is based on solving the conservation laws for mass, momentum, and energy, is the only existing approach that has any hope to be generally applicable to indoor spreading of chemical, biological or radiological threat compounds. A wide range of CFD models are available with different complexity and predictive capabilities, cf. e.g. [3]. Even though the computational costs of CFD models are high, they offer great potential, in particular as valuable tools for planning, education, training, and other purposes not restricted to real-time dispersion assessments. Since the complexity of contaminant dispersion arises from interdependency of many complex physical processes, it is essential to establish an understanding of the fundamental relations among these and to determine leading order effects.

A thorough literature survey related to the mechanisms of indoor transport of contaminants was conducted by Gant et al. [4]. They consider both the indoor air environment and the characteristics of contaminants, and CFD simulations were conducted to simulate the indoor transport. Guerra et al. [5] studied the space-time evolution of pollutants from a jet into a closed area both with experiments and with CFD (standard  $k-\epsilon$  model). Based on this they proposed a simple model for indoor dispersion. The application of

\* Corresponding author at: Norwegian Defence Research Establishment (FFI), Protection Division, Instituttveien 20, P.O. Box 25, NO-2027 Kjeller, Norway. Tel.: +47 6380 7898; fax: +47 6380 7509.

E-mail addresses: [Monica.Endregard@ffi.no](mailto:Monica.Endregard@ffi.no) (M. Endregard), [Bjorn.Reif@ffi.no](mailto:Bjorn.Reif@ffi.no) (B.A. Pettersson Reif), [Thomas.Vik@ffi.no](mailto:Thomas.Vik@ffi.no) (T. Vik), [Odd.Busmundrud@ffi.no](mailto:Odd.Busmundrud@ffi.no) (O. Busmundrud).

<sup>1</sup> Also: University of Oslo, Dept. of Mathematics, NO-0316 Oslo, Norway.

this model is bound by the parameter range of the experiments and simulations. They continue this work by studying the effect of room ventilation (among more). Salim et al. simulated the dispersion of pollutants evaporating from a liquid surface in a closed room this with the standard  $k-\varepsilon$  model [6]. Although they focused mostly on source modelling (evaporation), they also concluded that the geometry of the room and the position of the air supply diffusers primarily determine the airflow. Reinke and Brosseau [7] modelled a similar scenario with a well-mixed box model modified for short-circuiting where the air jet enters the room. Lee et al. [8] simulated the dispersion of tracer gas from a source inside a room using the Reynolds Averaged Navier–Stokes (RANS) approach and compared the simulation with experimental measurements. They emphasise the importance of considering the velocity profile of the inlet air when conducting CFD simulations of the dispersion in closed spaces. This is especially important in relatively small confined spaces. Reynolds [9] compared experimental measurements of the concentration of a tracer gas in a full-scale building, with calculated concentrations from the Thomson's model (which satisfies the well-mixed condition for Gaussian turbulence) coupled with the standard  $k-\varepsilon$  model. He stresses that it is not appropriate to use simple models (for instance simple diffusion models) for predicting particle dispersion in flows with strong mean-streamline straining; instead sophisticated Lagrangian stochastic models of turbulent dispersion should be used.

The application of CFD in dispersion modelling is dominated by the RANS approach. In this study, however, the Large Eddy Simulation (LES) approach is adopted. The LES approach is in general more computationally expensive than RANS, but the large scale temporal variations and the meandering of the spatial scales of the turbulence are naturally accounted for even in statistically steady flow fields. These processes are very important within the context of transport of contaminants. Large scale unsteady mixing can also be captured by the unsteady RANS approach (URANS), but only for statistically unsteady flow fields.

## 2. Scenario description

### 2.1. Sarin properties and toxicity

The nerve agent sarin (isopropyl methylphosphonofluoridate) is an odour- and colourless liquid in its pure form at ambient conditions (boiling point 147 °C) [10]. Sarin was produced and stockpiled as a chemical warfare agent by several countries after the Second World War. All parties to the Chemical Weapons Convention (CWC) have destroyed, or are in the process of destroying, their chemical stockpiles. Sarin has no industrial use and is not commercially available. However, the compound can be obtained by chemical synthesis if the actors have the necessary competence and available appropriate precursor chemicals, laboratory facilities and personal protection gear. Purchase of the most important precursor chemicals is governed by export control measures in accordance with the CWC and the Australia Group Export Control list. This constitutes a hurdle for possible perpetrators, but could unfortunately be circumvented.

**Table 1**  
Toxicity estimates for sarin for the 70 kg human.

Toxicity	Route and form of exposure	Exposure time (min)	Estimated value (mg min/m <sup>3</sup> )	Minute volume (l min <sup>-1</sup> )	Reference
EC <sub>50</sub> <sup>a</sup>	Inhalation and ocular, vapour	2–10	2	–	[4]
LC <sub>50</sub> <sup>b</sup>	Inhalation, vapour	2	36	15	[6]
LC <sub>50</sub> <sup>b</sup>	Inhalation, vapour	10	57	15	[6]
LC <sub>50</sub> <sup>b</sup>	Inhalation, vapour	30	79	15	[6]

<sup>a</sup> The inhalation dose that for exposure time,  $t$ , causes mild effects (miosis or rhinorrhea) in 50% of the exposed population.

<sup>b</sup> The inhalation dose that for exposure time,  $t$ , produces lethal effects in 50% of the exposed population.

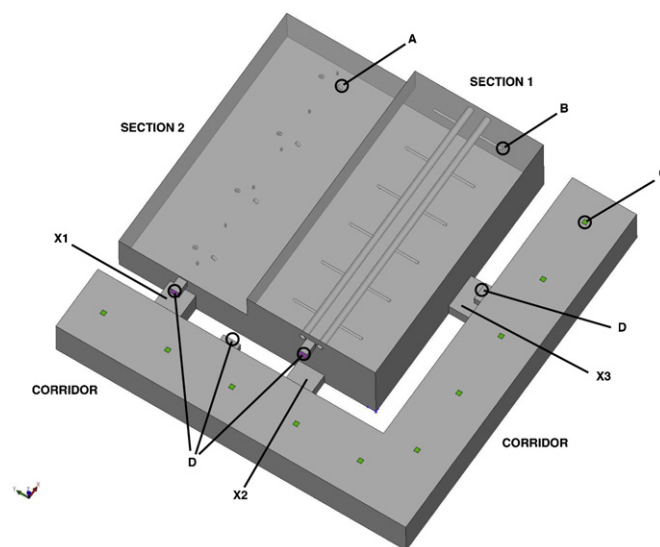


**Fig. 1.** Schematic of building complex: (A) supply of fresh air to section 2 (in total 14 inlets with  $A_{\text{inlet}} = 0.181 \text{ m}^2$  each); (B) supply of fresh air to section 1 (in total 19 inlets with  $A_{\text{inlet}} = 0.071 \text{ m}^2$  each); (C) supply of air to corridor (in total 10 inlets with  $A_{\text{inlet}} = 1 \text{ m}^2$  each); and (D) outlet ducts (one from each section and two from the corridor). The exits from sections 1 and 2, respectively, to the corridors are marked by X1–X3.

Sarin is an organophosphate compound, and its highly toxic properties stem from the inhibition of the enzyme acetylcholinesterase [10,11]. It constitutes an inhalation hazard if dispersed as aerosol or vapour, but can also be absorbed through the skin and pose a severe risk by intake of contaminated foodstuff. This class of nerve agents blocks the effects of acetylcholinesterase at the myoneural junction, leading to overstimulation of the cholinergic receptors by excessive levels of the neurotransmitter acetylcholine. Symptoms of intoxication are impaired vision (pin-point pupils, i.e. miosis), dizziness, headache, vomiting, runny eyes and nose, bloody secretion from mouth, diarrhoea, fasciculations, convulsions, then respiratory arrest and death [12]. The onset of symptoms upon inhalation is rapid (minutes). Bide et al. [13] have recently provided human sarin toxicity estimates recommended for the general population based on a reassessment of animal inhalation toxicity data. Some of these estimates have been used in the consequence assessment in this study (Table 1).

Medical treatment of organophosphate intoxication includes administration of three drugs, preferably within minutes after exposure: an anticholinergic drug (atropine), a re-activator of the inhibited acetylcholinesterase (oximes, e.g. pralidoxime or obidoxime) and anticonvulsive therapy (benzodiazepines) [12,14]. Many countries have auto-injectors for this purpose for their military service, and sometimes also for civilian use by first responders.

### 2.2. Building technical description

The hall consists of two sections, each 1800 m<sup>2</sup>, which vary in height (cf. Fig. 1 for details); section 1 has a height of 16.6 m, section

2 a height of 9.8 m. There is no wall separating the sections. There are two exits from section 1 to the corridor (exit X2: 3 m × 6 m and exit X3: 3 m × 8 m, respectively) and one exit (X1) from section 2 to the corridor (dimension 6 m × 5.5 m). In addition, there are gates at the opposite walls that can be opened and used in crisis situations for evacuation of people. The evacuation gates are assumed to remain closed during the scenario, whereas all three passages between the main halls and the corridor (X1–X3) remain fully open.

The ventilation system consists of three individually operated systems for sections 1, 2, and the corridor, respectively. For each system, fresh inlet air from the outside passes through a heat exchanger before being distributed inside the building. Immediately downstream the heat exchanger, the temperature controlled air passes through a 1 m × 1 m square straight duct which is accessible through an inspection door. Due to the large number of people present in the building complex, the ventilation system is assumed to operate close to full capacity with an air mass flow rate of 15.1 kg/s. It is assumed that all three ventilation systems are operated individually in a fully balanced configuration (i.e. mass flow rate in = mass flow rate out) and with no external leakages caused by open doors or windows. The ventilation system consists of 19 circular inlets in section 1 (each with an area 0.071 m<sup>2</sup>), 14 rectangular inlets in section 2 (8 with an area 0.25 m<sup>2</sup> and 6 with 0.09 m<sup>2</sup>), and 10 squared inlets in the corridor (1 m<sup>2</sup>). The velocity and scalar fields were simply specified on the cross sectional area at the inlet exits, i.e. the computations do not account for the internal shapes of the ventilation other than the shape of the inlet nozzles.

### 2.3. Source and release characteristics

We assume that actors break into the main ventilation control room. A bottle of sarin containing 420 g is emptied in the ventilation duct for section 1 immediately downstream the heat exchanger. The wind speed in the shaft is 12.5 m/s, and the temperature is 16 °C. It is assumed that sarin (liquid density 1.09 g/cm<sup>3</sup>) forms a liquid pool (area of 1 m<sup>2</sup>, depth 0.4 mm) inside the ventilation duct. Sarin evaporates and mix with the inlet air for section 1.

### 3. Dispersion modelling

The terminology ‘dispersion modelling’ alludes in the present work both to source characterization and transport modelling. The former involves an estimate of the evaporation rate, and subsequent mixing with the airflow, within the internal parts of the ventilation system before the air exits through the ventilation inlets inside the building. The transport model describes the dispersion of air containing sarin vapour from the ventilation inlets to the building interior. While the air from the inlets in section 1 is contaminated by sarin, fresh air is continuously distributed from the inlets close to the ceilings in section 2 and the corridor, respectively.

The rate of evaporation from a liquid pool is affected by a wide range of chemical and physical processes. First and foremost the vapour pressure and the exposed surface area of the evaporating liquid pool are crucial. Furthermore, the molecular weights (of the substance and the surrounding media), the ambient temperature, and the overall pressure affect the evaporation rate. A temperature difference between the liquid and the ambient media leads to temperature gradients that influence the rate of evaporation. In this case, however, due to the low vapour pressure of sarin, isothermal conditions can be assumed. In addition, properties of the airflow above the pool are important. The air stream above the pool efficiently transports vapour downstream thereby reducing the local concentration level above the pool’s surface. This increases the vertical concentration gradient which subsequently increases the evaporation rate.

The sources inside the building in the present case are uniformly distributed close to the ceiling in section 1, and it would thus be plausible to use a simple empirical ventilation model, cf. e.g. [15], to compute the contaminant dispersion in that part of the building. The source characterisation is however very different in the two remaining parts of the building. The rate at which contaminated air enters section 2 and the corridor, respectively, depends on the time varying contaminant transport within section 1. This a priori unknown source of contaminants is very important in the present case study since a large number of people are expected to be presented also in these parts of the building. The results in the present study are therefore obtained from CFD models.

Release through the ventilation system is generally classified as jet (or momentum) controlled flows, cf. e.g. [4]. The airflow from the ventilation inlets is under most conditions fully turbulent, and the entrainment and diffusion processes significantly increase the mixing and dilution of contaminants. In the present scenario, the ventilation system is assumed to be working with near-full capacity due to the large number of persons present indoor. The speed of the contaminated air exiting through the inlets is therefore relatively high (Re ≈ 100,000 based on the diameter of the ventilation inlet). It can be anticipated that the flow becomes unsteady due to the interaction between the jets close to the floor (due to the radial impinging jets) and will therefore exhibit an unsteady meandering motion, at least within the time scale of the present release (which cannot be considered as continuous). As a result, slowly varying large scale unsteady motions throughout the convention centre are expected, but it should be pointed out that the flow field remains essentially statistically steady. This unsteadiness is a crucially important feature of the dispersion from multiple ventilation inlets in large spaces. The most notable effect of this unsteadiness on the dispersion process in this case is related to the transport of sarin from section 1, where the release takes place, to section 2 and the corridor, respectively. The most common CFD approach for turbulent fluid flows is based on the RANS approach; these can also in principle account for unsteady mixing, but only in cases where the flow field is statistically unsteady. The more computationally expensive Large Eddy Simulations (LES) approach has therefore been adopted in the present case.

The LES approach is based on the filtered Navier–Stokes equations:

$$\frac{\partial \tilde{u}_i(\mathbf{x}, t)}{\partial t} + \tilde{u}_k(\mathbf{x}, t) \frac{\partial \tilde{u}_i(\mathbf{x}, t)}{\partial x_k} = -\frac{1}{\rho} \frac{\partial \tilde{p}(\mathbf{x}, t)}{\partial x_i} + \nu \nabla^2 \tilde{u}_i(\mathbf{x}, t) - \frac{\partial \tau_{ij}(\mathbf{x}, t)}{\partial x_j},$$

governing the filtered velocity field

$$\tilde{u}_i(\mathbf{x}, t) = \frac{1}{V} \iiint u_i(\mathbf{x}', t) G(\mathbf{x}', \mathbf{x}) d\mathbf{x}'.$$

Here  $u_i(\mathbf{x}, t)$  is the velocity components,  $G(\mathbf{x}', \mathbf{x})$  is the filter function,  $\rho$  is the density,  $\nu$  is the kinematic viscosity, and  $\tau_{ij}$  is the residual stress tensor (see Section 3.2).

Sarin in vapour form can to a good approximation be treated as a passive scalar, i.e. a scalar quantity that is passively transported without affecting the airflow itself. The scalar field (of sarin),  $c = c(\mathbf{x}, t)$ , is obtained by solving the equation:

$$\frac{\partial c(\mathbf{x}, t)}{\partial t} + \tilde{u}_i(\mathbf{x}, t) \frac{\partial c(\mathbf{x}, t)}{\partial x_i} = \frac{\partial}{\partial x_i} \left( \kappa \frac{\partial c(\mathbf{x}, t)}{\partial x_i} \right),$$

where the molecular diffusivity is denoted by  $\kappa$ . In order to simplify the modelling, a number of assumptions are invoked: (i) the physical presence and movement of persons are neglected, (ii) isothermal conditions are assumed, and (iii) the rate of deposition on walls is neglected. It is believed that the effect of neglecting these processes is secondary as compared to the effect on scalar transport and mixing due to turbulent air motion. It should be noted that

the physical effect of the two first processes is to increase the local mixing in the region closest to the floor and thereby also increase the homogeneity of the turbulence, i.e. a tendency to render the local mixing more uniformly distributed. Neglecting these effects may result in local differences in the concentration levels, but since the analyses performed in the present study are solely based on the area-weighted and time averaged results (averaged in a horizontal plane parallel 1 m above the floor are shown), it is believed the impact of these simplifying assumptions are secondary.

### 3.1. Source modelling

A model for estimating the evaporation rate from a liquid pool has been developed at FFI. It is assumed that the liquid forms a pool on a flat surface, and that air flows parallel to the surface, with zero speed within a thin layer of thickness  $\delta$ . Further out the velocity is constant ( $v_x$ ). If all mass transport in the wind-free zone is due to diffusion, and if the concentration of the diffusing vapour is zero at  $\delta$  (all vapour is carried away by the air stream), then from Fick's law for steady-state diffusion, the following expression for the evaporation rate is found:

$$J = \kappa \frac{C_0(T)}{\delta} A,$$

where  $C_0(T)$  is the saturation vapour concentration,  $T$  is the temperature at the liquid surface (assumed equal to the air temperature),  $\kappa$  is the molecular diffusion coefficient and  $A$  is the surface area of the pool.

Hummel et al. [16] give the following formula for the diffusion coefficient of a vapour  $A$  in a gas  $B$  (dimension  $\text{m}^2/\text{s}$ ):

$$\kappa_{AB} = \frac{4.14 \times 10^{-4} T^{1.9} \sqrt{(1/MW_B) + (1/MW_A)} (MW_A)^{-0.33}}{p},$$

where  $MW_A$  and  $MW_B$  are the molecular weights of chemical  $A$  and  $B$ , respectively (in  $\text{g/mol}$ ) and  $p$  is the ambient pressure (in  $\text{Pa}$ ).

The vapour concentration is calculated from the vapour pressure ( $p_0$ ) by:

$$C_0 = \frac{p_0 \cdot MW}{RT},$$

where  $R$  denotes the gas constant. An empirical expression for the diffusion length,  $\delta$ , is determined from experimental measurements of the evaporation rate for a number of substances as function of the speed of air  $v_x$  (in  $\text{m/s}$ ):

$$\delta = 1.6 \times 10^{-3} v_x^{-0.7}.$$

### 3.2. Transport modelling

The LES modelling capability of the commercial software FLUENT was utilized in the present study. The Smagorinsky–Lilly dynamical sub-grid stress model was used on a computational grid consisting of approximately 1.8 million cells. The spatial resolution of the grid was 0.5 m everywhere except in section 1 where a grid refinement was performed in order to ensure that the rapid spatial variations of the flow field in the vicinity of the ventilation inlets and outlets, respectively, were captured. In these regions, the grid resolution was approximately 0.1 m close to the inlet and 0.25 m close to the outlets. The 0.5 m resolution has been judged sufficient to capture the large scale meandering motion of the jets close to the floor – a phenomena occurring at spatial scale in the order of 5–10 m. Second order time implicit and bounded central difference schemes were used. The time step was set to 0.3 s, and approximately 10 sub-iterations were needed to reach numerical convergence levels less than 0.0001 for each time step. This implies e.g. that the overall numerical error for the  $x$ -velocity

component is four orders of magnitude less than the corresponding bulk  $x$ -momentum in the system. No-slip boundary conditions were applied on all solid surfaces and the inflow and outflow conditions were based on a specified mass flow (15.1 kg/s for each individual ventilation system). It should be noted that the inherent unsteadiness observed in the computations is due to the interaction of the jets impinging on the floor, and not the unsteadiness due to turbulence within the ventilation system itself.

The a priori unknown residual stress tensor in the filtered Navier–Stokes equations is modelled using the dynamic Smagorinsky–Lilly model, i.e.

$$\tau_{ij} \equiv \widetilde{u_i u_j} - \widetilde{u_i} \widetilde{u_j} = \frac{1}{3} \widetilde{u_k u_k} \delta_{ij} - 2\nu_T \widetilde{\xi}_{ij},$$

$$\nu_T = L_s^2 |\widetilde{\xi}| = \min(0.41d, C_s V^{1/3})^2 \sqrt{2\widetilde{\xi}_{ij} \widetilde{\xi}_{ij}},$$

$$\widetilde{\xi}_{ij} = \frac{1}{2} \left( \frac{\partial \widetilde{u}_i(\mathbf{x}, t)}{\partial x_j} + \frac{\partial \widetilde{u}_j(\mathbf{x}, t)}{\partial x_i} \right).$$

Here,  $d$  and  $V$  denotes the distance to the nearest solid surface and volume of the computational cell. The model coefficient  $C_s$  is determined by the solution itself by using a test filter, cf. Pope [17] for details.

In order to establish a realistic flow field at the initiation of the release, 400 time steps were conducted in which only fresh air exited through the inlets. At the time of release  $t = t_0$ , the sarin concentration level at each of the 19 ventilation inlets in section 1 was specified according to the source model. The velocity and scalar fields then evolved simultaneously in time until  $t_1 = t_0 + 20$  min, when according to the source model all sarin had evaporated and the release stopped. Then the ventilation system again provided fresh air, and the computations continued for another 30 min.

## 4. Results and discussion

### 4.1. Source and dispersion modelling results

The estimated evaporation rate, using parameters in Section 2.3 and the model described in Section 3.1, is approximately 0.35 g/s, such that the entire pool will evaporate in 20 min.

The flow inside the convention hall is in this case inherently unsteady since it is dominated by momentum transfer at very high Reynolds numbers. This unsteadiness reveals itself in large scale flow patterns with time scale  $\sim O(10)$  seconds. Since the release continued over a time interval (20 min), time averaging of the results is not appropriate. The formally correct way to conduct averaging, and to subsequently be able to describe the flow as statistically steady, is by conducting an ensemble averaging. This would require several hundreds of independent LES runs and is scarcely feasible. It should also be noted that instantaneous fluctuations of momentum (and concentration) may exhibit maxima that could be very important and different from an averaged value.

Figs. 2–4 display snapshots of the instantaneous velocity (vectors) and concentration (contour) fields in a plane 1 m above the floor at different times. It is interesting to note that the concentration levels at the latest snapshot in this time series (Fig. 4) are generally higher in section 2 than in section 1.

The results presented here are area-weighted concentrations based on an average of the instantaneous concentration field 1 m above the floor level, i.e.  $\bar{c}(t) = \iint c(t) dA/A$  where  $A$  is the total horizontal area in each of the three main areas of the building, respectively. The corresponding dosage,  $d(t) = \int_0^t \bar{c}(t') dt'$ , is also computed in each of the different areas of the building, i.e. sections 1, 2, and the corridor, respectively.

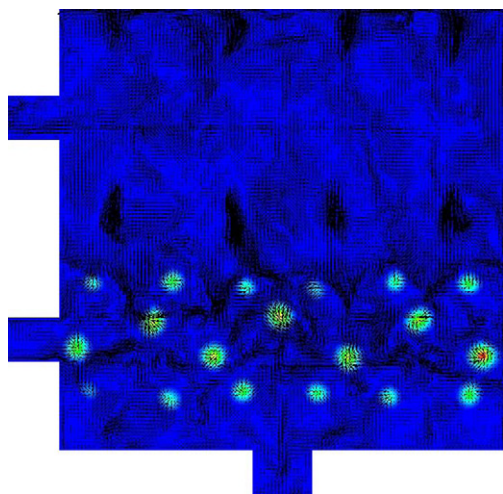


**Fig. 2.** Instantaneous velocity (vectors) and concentration (contour) fields in a horizontal plane 1 m above the floor in sections 1 and 2, respectively, immediately after start of release. Red: high concentration level; blue: low concentration level. (For interpretation of the references to colour in this figure legend, the reader is referred to the web version of the article.)

A number of simplifying assumptions have been made. We have not taken into account structures and objects such as furniture and partitioning walls, the movement of people in the convention hall, which locally would affect the concentration levels at floor level, and the effect of heating due to people. These effects, however, all have the tendency to locally increase the mixing at floor level by enhancing the level of turbulence fluctuations. Since the large scale fluid motion above the immediate vicinity of the floor, that is primarily responsible for the transport of sarin vapour across the convention centre, is predominately driven by the momentum flux through the ventilation inlets, it is not expected that the locally enhanced mixing very close to the floor plays a significant role on the overall transport. Since the inhaled dose of sarin is dependent on the time integral of the concentration, short-term local concentration variations will be levelled out as far as the consequence of the poisoning is concerned.

Given the above simplifications, the resulting area-weighted concentrations and doses of sarin 1 m above the floor are shown

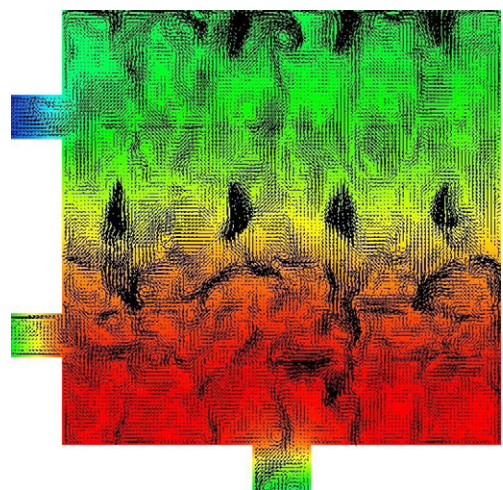


**Fig. 3.** Instantaneous velocity (vectors) and concentration (contour) fields in a horizontal plane 1 m above the floor in sections 1 and 2, respectively, approximately 10 min after start of release. Red: high concentration level; blue: low concentration level. (For interpretation of the references to colour in this figure legend, the reader is referred to the web version of the article.)

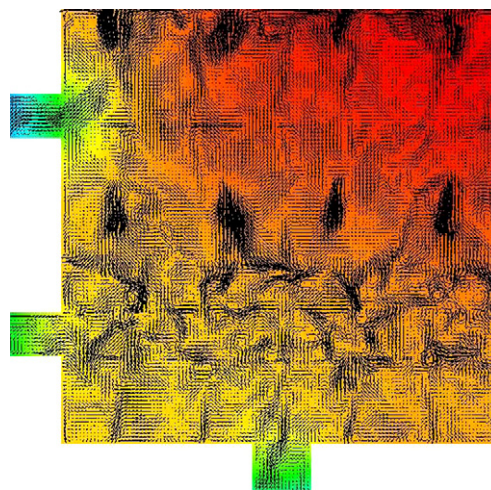


**Fig. 4.** Instantaneous velocity (vectors) and concentration (contour) fields in a horizontal plane 1 m above the floor in sections 1 and 2, respectively, approximately 40 min after release. Red: high concentration level; blue: low concentration level. (For interpretation of the references to colour in this figure legend, the reader is referred to the web version of the article.)

in Figs. 5 and 6, respectively. In Fig. 6 we have added three toxicity sarin estimates ( $LCt_{50}$ , ref. [13]) with a second order polynomial between the estimates. In section 1, a dose corresponding to  $LCt_{50}$  is reached after 19 min, while in section 2 this dose is reached after 27 min. Tables 2 and 3 display the average concentrations and doses, respectively, at selected elapsed times after release.

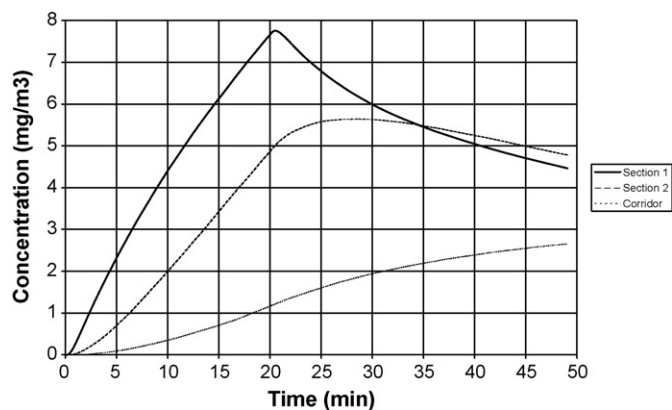


**Fig. 5.** Average concentrations of sarin 1 m above floor level in sections 1, 2, and the corridor, respectively.

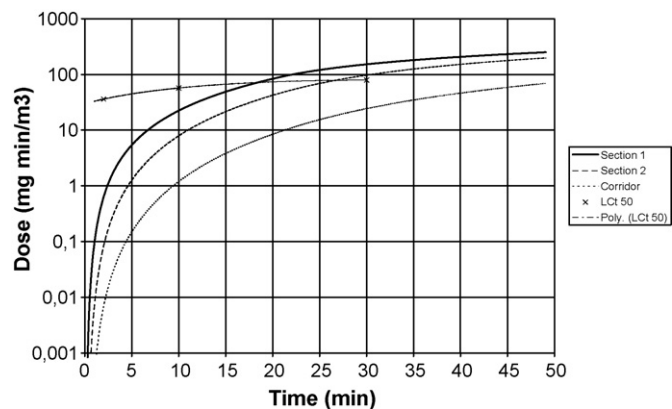


**Fig. 6.** Average doses of sarin as a function of time, at 1 m above floor level in sections 1, 2, and the corridor, respectively.

**Table 2**

Average concentrations ( $\bar{c}$ ) at 1 m above floor level after selected times ( $t$ ) after release of sarin in sections 1, 2 and the corridor, respectively.

$t$ (min)	$\bar{c}$ (mg/m <sup>3</sup> )		
	Section 1	Section 2	Corridor
4	1.8	0.5	0.1
10	4.4	2.0	0.4
20	7.7	4.9	1.2
30	6.0	5.6	1.9
50	4.5	4.8	2.7

**Table 3**

Average dose ( $d$ ) at 1 m above floor level at selected elapsed times ( $t$ ) after release of sarin in sections 1, 2 and the corridor, respectively.

$t$ (min)	$d$ (mg min/m <sup>3</sup> )		
	Section 1	Section 2	Corridor
4	3.4	0.7	0.1
10	22	7.9	1.2
20	84	42	8.4
30	152	97	24
50	250	197	69

**Table 4**

Possible consequences based on calculated doses (Ct) and toxicity estimates in Table 1.

Possible consequences	Elapsed time after release		
	Section 1	Section 2	Corridor
50% of the exposed population experience mild effects, i.e. pin-point pupils (miosis) and rhinorrhea	3 min	6 min	12 min
50% of the population exposed to lethal dose	19 min	27 min	–

Note that the concentration in the corridor continues to increase long after the release in section 1 ceased. The dispersion simulation dataset can be scaled and used for other types and amounts of released passively transported contaminants under the assumption that the release is continuous for 20 min.

#### 4.2. Consequence assessment

Table 4 gives possible time evolution of intoxication symptoms using the calculated doses in Fig. 6 and the acute sarin toxicity estimates in Table 1. It is assumed that people are uniformly distributed and do not escape. In practice this will not occur, however it is difficult to predict reaction patterns, and it gives an indication of possible scenario development.

For estimating casualty numbers one can assume that a total number of 1200 persons are present: 500 persons in section 1, 500 persons in section 2, and 200 persons in the corridor. Mild effects appear within minutes for hundreds of persons, while serious injuries and fatalities occur approximately 20 min after release. The results show that the consequences may be more severe in the present case as compared to the outcome of the sarin release in the Tokyo subway. Factors that may have contributed to predominantly mild cases and relatively low number of immediate deaths in 1995 were that sarin in a diluted form was released, that the release mechanism was not very efficient, and due to the high efficiency of the ventilation system in the Tokyo subway system [1,18].

It is assumed that the release is covert, no sound is heard, and no detectors are in place. Since sarin is odourless and colourless in its pure form, the first alarm will be people experiencing symptoms of nerve agent poisoning. In this case, the timeline from onset of early symptoms until inhalation of a lethal dose is short (approx-

mately 16 min in section 1), which gives limited time to evacuate and mitigate the consequences.

Exhibition equipment and furniture at floor level will make it difficult to obtain an overview of the situation. It will probably take some time until the severity of the event will be understood and organised evacuation initiated. Some persons will self-evacuate upon early symptoms, while others will suspect heart attacks for persons keeling and seek to assist them. Due to the rapid dispersion of contaminated air through the ventilation system and effective distribution of air in the hall, the casualty numbers will increase rapidly. Consequently, the first responders will most likely face a large number of seriously injured and several fatalities.

## 5. Emergency management challenges

This hypothetical scenario poses severe challenges for the emergency response services due to the high number of casualties caused by an unknown toxic chemical. Important questions are: When and how will alarm be raised? Who will be called? Who will be the first on the scene? What are the anticipated response times? How will first responders be organised? Who will be in charge? How will responders be equipped (personal protection equipment, detectors, medical countermeasures, decontamination equipment, etc.)? Will other services and resources be called upon? How will people be evacuated to hospitals? Is there a need for decontamination of casualties to avoid secondary contamination and exposure, and if so how will this be accomplished? Are necessary drugs for medical treatment available in the required quantities? How will the causative agent be detected and identified? Is there a need for international assistance, and if so, how can it be provided in a timely manner? Some of these questions are addressed and discussed below.

### 5.1. Alarms and response times

Since no other indication of the event occurs, the first alert will most likely be observation of symptoms of nerve agent poisoning. Early symptoms may resemble that of a heart attack or asthma, thus the first phone call will probably report medical emergencies. Due to the magnitude of the incident, the emergency centrals may quickly suspect release of poisonous gas and alert all blue light services. Some people will panic and flee, some will evacuate calmly, and some will seek to assist those suffering severe poisoning. Ambulances, police and fire brigade are expected to arrive quickly at the incident scene (in densely populated areas usually within 5–20 min).

### 5.2. Rescue operations

The main priorities in the early phase are to save lives by evacuating victims and providing first aid and life-saving medication, and at the same time maintain the safety of the rescue personnel. Unprotected rescue personnel may themselves become casualties. The key challenge for the Incident Commander is to define safety zones and placement of the command control post; decisions that necessarily will be based on limited factual information, but which are crucial safety precautions for emergency personnel and the public. The availability and type of individual protective equipment vary both between the services, and between countries and regions. In many cases the police and medical emergency personnel will not have personal protective equipment available, such as respirators, protective garments and detectors. The fire brigade's smoke divers, however, are equipped with self-contained breathing apparatus and fire fighter's garment, and hence are protected against inhalation hazards. The chemical divers are protected against toxic chemicals both in vapour and liquid form, since they too are

equipped with self-contained breathing apparatus, and in addition impermeable chemical suits. Some fire departments have chemical agent detectors capable of detecting nerve agent vapour. The fire brigade has decontamination equipment intended for its own personnel, and will establish a decontamination post at the entry/exit point to the hot zone. At hazardous materials events, the fire brigade is usually the only service operating inside the hot zone. The fire brigade will seek to mitigate further dispersal of toxic chemicals by covering the source or sealing the chemical leak, thereby avoiding further release and exposure of personnel.

A key question will be whether life-saving medication (auto-injector administration of atropine and oxime) can be provided to patients who have not undergone decontamination. The time aspect is crucial, and the most difficult part will be to rescue persons suffering from nerve agent poisoning. Administration of drugs at an early stage is a prerequisite. Treatment should commence as quickly as possible, but will in many cases not be given since health-care workers may not have the necessary personal protection to assist possibly contaminated victims.

### 5.3. Decontamination of victims

Upon release of hazardous substances it is vital to stop further exposure of victims and avoid secondary exposure cases. Therefore, many emergency services have adopted the following rules of thumb: Ambulances will only transport clean patients, and hospitals will only admit patients after decontamination (removing clothes and showering), either at the scene or at the hospital. This is based on experience and recommendations from hazmat incidents and the sarin attack in Tokyo, where drivers and medical staff experienced symptoms due to vapour exposure from contaminated patients [18–21].

The logistics regarding decontamination of victims in mass casualty hazmat incidents is under debate [22]. Decontamination at the mass casualty incident scene using mobile decontamination units is time-consuming and will delay critical medical treatment. The most important step to avoid further exposure of the victim, cross-contamination, and exposure of others is to remove all clothing and personal belongings and secure these items in sealed containers. Levitin et al. [22] state that this is the minimum acceptable level of decontamination, and for vapour exposure it may be the only action needed. This step can be performed at the scene, but must be done as quickly as possible. Also, efficient ventilation is an important precautionary measure. A complicating factor in many cases is that the contaminant is neither visible nor detectable by smell or detectors, and it may therefore be difficult to decide whether the person has been exposed to liquid or only vapour.

### 5.4. Detection and identification

A key point is as quickly as possible to establish the causative agent. Detectors operated by first responders may provide a first indication that the toxic compound in this case is an organophosphate. Medical doctors may recognise organophosphate poisoning and administer appropriate drugs based on observed symptoms. In this case, and for many other toxic compounds, identification by laboratory analysis of collected samples is the only way to unambiguously identify the toxic chemical. Identification is important to initiate optimal medical treatment for victims, and to make correct decisions concerning mitigating measures and to normalise the situation at the hazard scene. Also, unambiguous identification is a cornerstone of forensic work and subsequent trials against the perpetrators. Samples from the scene or exposed victims should be sent for analysis at laboratories. In previous cases, sarin and sarin hydrolysis products were identified [1,23]. Designated laboratories by the Organisation for the Prohibition of Chemical Weapons exist,

and many countries have defence laboratories with expertise, laboratory facilities, and established analysis techniques and methods. Detection, sampling, and identification will also be important in the restoration phase to identify the need for decontamination and verify absence of contamination when preparing the building for normal use. In this scenario, since the entire amount of sarin in the ventilation shaft will evaporate, decontamination of the building will probably not be necessary, other than possibly for psychological reasons.

### 5.5. Overload of the health system

Persons with nerve agent poisoning require treatment and medication in relatively large doses for days or sometimes months [14]. There may be a shortage of stockpiled medical supplies, and it may be necessary to purchase from commercial suppliers or receive drugs as assistance from other countries. A request for international assistance regarding intensive care for seriously intoxicated patients may also be issued if there is insufficient capacity at national hospitals.

Ambulatory patients with light symptoms will probably self-evacuate and leave the scene to seek medical treatment by own means before the area has been cordoned off. For example, after the Tokyo attack, the vast majority of the 5000 persons seeking medical attention used other means of transportation to hospitals than ambulances or fire brigade vehicles [18,19]. The present hypothetical scenario will probably result in rapid overload of health services, which could endure for a week or more [24]. Of these persons, many, perhaps the majority, only suffer from perceived exposure (“worried-well”). The healthcare workers will face the difficult and time-consuming challenge to separate patients with mild symptoms from those with stress-related or no symptoms who have concerns and request information. Laboratory evaluation may be available to confirm exposure. Hendrickson [24] refers to several mass psychogenic illness episodes caused by chemical releases, thus health care facilities should prepare for this. Another point is to prepare for follow-up of victims in the long-term to examine possible long-term health consequences [25].

## 6. Conclusions

In addition to lessons learned from historical incidents, construction and analysis of hypothetical scenarios are recommended as tools for emergency response planning, education, training, and exercises. In this study, a hypothetical scenario of indoor release of the highly toxic chemical sarin through the ventilation system is presented. The scenario has been simulated using a CFD approach in order to ensure realistic concentration profiles versus time. Primary objectives in any crisis situation are to save lives, rescue persons, and to secure the area. In the present scenario three factors complicate emergency response: (i) time, (ii) large number of casualties, and (iii) contaminated victims and hazard scene. This scenario can be used by central, regional and local authorities, first responders, civil defence units, hospitals, military units, and other organisations to discuss and define roles and responsibilities in handling such incidents. A particular important challenge is inter-agency education and training to ensure effective crisis management and sufficient cooperation.

## Acknowledgements

The authors acknowledge support from the Norwegian Research Council through the Norwegian Centre of Excellence – Centre for Biomedical Computing.

## References

- [1] A.A. Tu, Chemical Terrorism: Horrors in Tokyo Subway and Matsumoto City, Alaken, Inc., Fort Collins, CO, 2002.
- [2] Planning Scenarios, Executive Summaries, The Homeland Security Council, July 2004, <http://www.globalsecurity.org/security/library/report/2004/hsc-planning-scenarios-jul04.exec-sum.pdf> (accessed 6 August 2008).
- [3] P.A. Durbin, B.A. Pettersson Reif, Statistical Theory and Modelling for Turbulent Flows, John Wiley & Sons, Ltd., 2001, ISBN 0 471 49744 4.
- [4] S.E. Gant, A. Kelsey, N. Gobeau, Factors Influencing the Indoor Transport of Contaminants and Modelling Implications, Report HSL/2006/29, Health and Safety Laboratory, Harpur Hill, Buxton, UK, 2006.
- [5] D. Guerra, L. Ricciardi, J.C. Laborde, S. Domenech, Predicting gaseous pollutant dispersion around a workplace, *J. Occ. Environ. Hyg.* 4 (8) (2007) 619–633.
- [6] S.M. Salim, S. Viswanathan, M.B. Ray, Evaluation of source model coupled computational fluid dynamics (CFD) simulation of the dispersion of airborne contaminants in a work environment, *J. Occ. Environ. Hyg.* 3 (12) (2006) 684–693.
- [7] P.H. Reinke, L.M. Brosseau, Development of a model to predict air contaminant concentrations following indoor spills of volatile liquids, *Ann. Occ. Hyg.* 41 (4) (1997) 415–435.
- [8] E. Lee, C.E. Feigley, J. Khan, An investigation of air inlet velocity in simulating the dispersion of indoor contaminants via computational fluid dynamics, *Ann. Occ. Hyg.* 46 (8) (2002) 701–712.
- [9] A.M. Reynolds, Modelling particle dispersion within a ventilated airspace, *Fluid Dyn. Res.* 22 (3) (1998) 139–152.
- [10] L.K. Engman, A. Lindman, A.-K. Tunemalm, O. Claesson, B. Lilliehöök (Eds.), Chemical Weapons—Threat Effects and Protection, FOI Briefing Book No. 2, FOI SE-172 90 Stockholm, Sweden, 2002, <http://www.foi.se>.
- [11] Review of acute human toxicity estimates for selected chemical warfare agents, in: L.D. Koller, D.E. Gardner, D.W. Gaylor, S. Green, R.F. Ender-son, B.M. Wagner (Eds.), Subcommittee on Toxicity Values for Selected Nerve and Vesicant Agents, National Academy Press, Washington, DC, 1997.
- [12] J. Newmark, Nerve agents: pathophysiology and treatment of poisoning, *Semin. Neurol.* 24 (2) (2004) 185–196.
- [13] R.W. Bide, S.J. Armour, E. Yee, GB toxicity reassessed using newer techniques for estimation of human toxicity from animal inhalation toxicity data: new method for estimating acute human toxicity (GB), *J. Appl. Toxicol.* 25 (2005) 393–409.
- [14] P. Aas, Future considerations for the medical management of nerve agent intoxication, *Prehosp. Disaster Med.* 18 (2004) 208–216.
- [15] H.E. Feustel, A. Rayner-Hoosen (Eds.), Fundamentals of the Multizone Air Flow Model—COMIS, Lawrence Berkeley National Laboratory, CA, USA, LBL report #28560, 1990.
- [16] A.A. Hummel, K.O. Braun, M.C. Fehrenbacher, Evaporation of a liquid in a flowing airstream, *J. Am. Ind. Hyg. Assoc.* 57 (1996) 519–525.
- [17] S.B. Pope, *Turbulent Flows*, Cambridge University Press, 2001, ISBN 0 521 59886 9 (pbk.), 0 521 59125 2 (hc.).
- [18] T. Okumura, N. Takasu, S. Ishimatsu, S. Miyanoki, A. Mitsushashi, K. Kumada, K. Tanaka, S. Hinohara, Report on 640 victims of the Tokyo subway sarin attack, *Ann. Emerg. Med.* 28 (2) (1996) 129–135.
- [19] T. Okumura, K. Suzuki, A. Fukada, A. Kohama, N. Takasu, S. Ishimatsu, S. Hinohara, The Tokyo subway sarin attack: disaster management, part 1: community emergency response, *Acad. Emerg. Med.* 5 (6) (1998) 613–617.
- [20] T. Okumura, K. Suzuki, A. Fukada, A. Kohama, N. Takasu, S. Ishimatsu, S. Hinohara, The Tokyo subway sarin attack: disaster management, part 2: hospital response, *Acad. Emerg. Med.* 5 (6) (1998) 618–624.
- [21] H. Nozaki, S. Hori, Y. Shinozawa, S. Fujishima, K. Takuma, M. Sagoh, H. Kimura, T. Ohki, M. Suzuki, N. Aikawa, Secondary exposure of medical staff to sarin vapor in the emergency room, *Intensive Care Med.* 21 (1995) 10323–11035.
- [22] H.W. Levitin, H.J. Siegelson, S. Dickinson, P. Halpern, Y. Haraguchi, A. Nocera, D. Turineck, Decontamination of mass casualties—re-evaluating existing dogma, *Prehosp. Disaster Med.* 18 (3) (2003) 200–207.
- [23] M. Nagao, T. Takatori, Y. Maeno, I. Isobe, H. Koyama, T. Tsuchimochi, Development of forensic diagnosis of acute sarin poisoning, *Leg. Med.* 5 (2003) S34–S40.
- [24] R.G. Hendrickson, Terrorist chemical releases: assessment of medical risk and implications for emergency preparedness, *Hum. Ecol. Risk Assess.* 11 (2005) 487–499.
- [25] T. Okumura, T. Hisaoka, T. Naito, H. Isonuma, S. Okumura, K. Miura, H. Maekawa, S. Ishimatsu, N. Takasu, K. Suzuki, Acute and chronic effects of sarin exposure from the Tokyo subway incident, *Environ. Toxicol. Pharmacol.* 19 (2005) 447–450.